Article

Distributed Optimal Control of DC Network Using Convex Relaxation Techniques

Yongbo Fu [1], Min Shi [2], Gongming Li [1], Zhangjie Liu [3,*], Juntao Li [1], Pengzhou Jia [1], Haiqun Yue [1], Xiaqing Liu [1], Xin Zhao [2] and Meng Wang [3]

[1] State Grid Handan Electric Power Co., Ltd., Handan 056011, China; fuyongbo@sgcc.com.cn (Y.F.); ligongming@sgcc.com.cn (G.L.); lijuntao@sgcc.com.cn (J.L.); jiapengzhou@sgcc.com.cn (P.J.); yuehaiqun@sgcc.com.cn (H.Y.); liuxiaqing@sgcc.com.cn (X.L.)

[2] State Grid Hebei Electric Power Co., Ltd., Shijiazhuang 050022, China; shimin@sgcc.com.cn (M.S.); zhaoxin@sgcc.com.cn (X.Z.)

[3] NARI Technology Nanjing Control Systems Co., Ltd., Nanjing 211106, China; wangmeng@sgcc.com.cn

* Correspondence: zhangjieliu@csu.edu.cn

Abstract: This paper proposes a novel distributed control strategy for DC microgrids using a convex relaxation method to ensure the system operates at the optimal power flow solution. Initially, a suitable convex relaxation technique is applied to transform the non-convex optimal power flow problem into a convex form, with the accuracy of this method being rigorously demonstrated. Next, the Karush–Kuhn–Tucker (KKT) optimality conditions of the relaxed problem are equivalently transformed, and a synchronization term is derived to facilitate the distributed control, thereby ensuring operation under optimal power flow. This paper also analyzes the impacts of communication delay and network structure on the performance of the proposed control strategy. Finally, simulations and numerical experiments are presented to validate the effectiveness of the proposed method.

Keywords: DC microgrid; distributed control; optimization; convex relaxation; second-order cone programming; stability

1. Introduction

In recent decades, to address the depletion of fossil fuels and reduce excessive reliance on them, efforts have been made to aggressively develop various emerging renewable energy sources, with solar and wind energy showing particularly promising growth. Unlike conventional power generation systems, renewable energy systems exhibit distinctive characteristics, complicating their integration into AC microgrids. In contrast, DC microgrids, with their advantages—such as the absence of reactive power, elimination of harmonics, simplified control, and reduced losses—are better suited for renewable energy systems [1–3].

The optimization control strategies for DC microgrids are primarily categorized into three types: decentralized, centralized, and distributed. In decentralized control, each node operates based on its own local information, resulting in a relatively simple control mechanism [4]. A common example of decentralized control is droop control [5]. The decentralized method avoids solving optimization problems that require real-time load information. Instead, it only needs to equalize the incremental cost using droop control. As a result, decentralized optimization methods can reduce costs without communication and achieve plug-and-play functionality. However, they are limited to simplified optimization models, such as neglecting cable resistance and the complex nature of currents. Furthermore, because they rely on droop control, these methods can result in significant deviations from the optimal operating point, particularly in large, complex systems, where the precise equalization of incremental costs is not achievable.

The centralized optimization control usually includes two core processes: The first is the centralized information processing process, in which the central controller collects data

from each controlled object or sensor for unified analysis and processing. The second is the decision-making and execution process; based on the processed information, the central controller formulates the control strategy, and issues specific control instructions to each controlled object to achieve the overall goal and performance requirements of the system [6]. When solving these optimization problems, centralized optimization methods often rely on traditional technical means, such as convex optimization methods [7] and heuristic optimization strategies. Due to low power constraints and voltage and current constraints, the ED problem is usually non-convex. To overcome this problem, some convex relaxation methods, such as the semi-definite programming [8] and second-order cone programming [9], are proposed. For the ED problem with more non-convex and stringent constraints, the heuristic optimization methods, such as the ant colony optimization [10], particle swarm optimization [11,12] and the deep neural network approach [13], are proposed to find the solution of the ED problem. The centralized control system relies on a central controller to interact with each node, enhancing system controllability and observability. However, this approach introduces challenges such as high communication load and reduced reliability.

Under distributed control, adjacent nodes communicate with each other to exchange information. This approach merges the benefits of both decentralized and centralized control while mitigating their respective drawbacks, resulting in improved performance. Several distributed consensus optimal methods are proposed to solve the ED problem, such as the distributed lambda-consensus algorithm [14,15], the distributed projected gradient method [16] and the alternating direction method of multipliers (ADMM) method [17,18]. Most of these methods turn the optimization problem into a convex problem by ignoring the complex characteristics of the power flow, and the obtained lambda-consensus conditions are not accurate and cannot reach the optimal solution. However, current distributed control strategies still fall short of achieving optimal control [19–21]. The distributed optimization method requires only low-bandwidth communication and is suitable for microgrids. The existing distributed optimization methods are more suitable for simple ED model distributed optimization methods, and ignore the complex power flow characteristics. Therefore, to achieve global economical dispatch, a more accurate optimal power flow model needs to be proposed by taking into account the characteristics of complex power flow.

This paper studies the optimal power flow of a DC microgrid model with resistive loads and proposes a distributed optimal control method to achieve optimal operation. Its main contributions are as follows:

(1) A semi-definite programming convex relaxation technique is proposed to transform the non-convex optimal power flow problem into a convex one, and it is proven that this convex relaxation is exact.

(2) The KKT condition is derived using the Lagrange multiplier method. Additionally, we convert the KKT optimality condition into a synchronization term that can be incorporated into the distributed control, ensuring the system operates at the optimal power flow solution.

(3) To achieve global optimality, global information is required, including all line resistances, loads, cost parameters, and so on. To further reduce communication costs, this paper proposes a distributed cost-optimization control strategy based on distributed observers. By using the distributed observer to obtain the global information, the method enables the calculation of optimal factors, allowing the controller to achieve voltage restoration and global optimal scheduling with only a sparse communication network. The impact of communication delays and the structure of the communication network on the performance of the proposed control strategy is also analyzed.

The paper is organized as follows: Section 2 introduces the key notations and defines the problem. Section 3 presents the main methodology and provides the relevant proofs. Section 4 discusses the simulations and validation of the proposed approach. Section 5 concludes the paper.

2. Related Works and Problem Formulations

Let $\mathbb{R}^n$, $\mathbb{R}^n_+$, and $\mathbb{R}^{n \times n}$ represent the sets of n-dimensional real vectors, n-dimensional positive real vectors, and $n \times n$ real matrices, respectively. For a vector $x \in \mathbb{R}^n$, $[x]$ denotes the corresponding diagonal matrix, while x^2 represents the element-wise square of x. The vector 1_n is an n-dimensional column vector of ones, and 0_n is an n-dimensional column vector, of zeros. If $x \in \mathbb{R}^n$ satisfies $x \geq 0_n$, it means that all elements of x are non-negative. For two vectors $x, y \in \mathbb{R}^n$, $x \leq y$ indicates that each element of x is less than or equal to the corresponding element of y. For a matrix $A \in \mathbb{R}^{n \times n}$, $A > 0$ and $A \geq 0$ imply that A is positive definite and positive semi-definite, respectively, while $A < 0$ and $A \leq 0$ indicate that A is negative definite and negative semi-definite, respectively.

2.1. The Existing Distributed Control Strategy in Microgrid

Consider a microgrid that comprises n dispatchable DGs. Typically, the operation cost function for the DC microgrid is expressed as follows:

$$f(p) = \sum_{i=1}^{n} f_i(p_i), f(p_i) = a_i p_i^2 + b_i p_i + c_i \tag{1}$$

where p_i and $f_i(p_i)$ represent the output power and the operation cost function of the i-th DG, respectively. a_i, b_i and c_i are coefficients that are all positive numbers. Subsequently, the optimization model for the ED adopts the following formulation:

$$\min_{p_i} f(p)$$
$$s.t. \sum_{i=1}^{n} p_i = p_{load} + p_{loss} \tag{2}$$

where p is the vector of p_i, p_{loss} is the line loss, and p_{load} is the equivalent total load power. Then, the Lagrangian operator for the optimization model is given by

$$L(p, \lambda) = f(p) + \lambda \left(p_{load} + p_{loss} - \sum_{i=1}^{n} p_i \right) \tag{3}$$

where λ is the Lagrangian multiplier about the equality constraint. Therefore, the KKT optimality condition of the optimization problem can be deduced as follows:

$$\begin{cases} \dfrac{\partial f_i(p_i)}{\partial p_i} - \lambda \left(1 - \dfrac{\partial p_{load}}{\partial p_i} - \dfrac{\partial p_{loss}}{\partial p_i} \right) = 0, \\ p_{loss} + p_{load} - \sum_{i=1}^{n} p_i = 0 \end{cases} \tag{4}$$

Then, assuming the dynamic value of load power and line loss power to each node power is 0, that is, $\partial p_{load} / \partial p_i = 0$ and $\partial p_{loss} / \partial p_i = 0$, the following KKT conditions are obtained:

$$\begin{cases} \dfrac{\partial f_1(p_1)}{\partial p_1} = \dfrac{\partial f_2(p_2)}{\partial p_2} = \cdots = \dfrac{\partial f_n(p_n)}{\partial p_n} = \lambda \\ p_{loss} + p_{load} - \sum_{i=1}^{n} p_i = 0 \end{cases} \tag{5}$$

Then, if (5) holds in the steady-state, the global optimal dispatch is achieved. Based on this idea, the λ-consensus [19] method is proposed in a distributed manner as follows:

$$u_i = \int \sum a_{ij}(\lambda_j - \lambda_i) dt + \int u_{ref} - \bar{u} dt \tag{6}$$

here, u_i denotes the instantaneous voltage of each distributed generator (DG), while $\lambda_i = \frac{\partial f_i}{\partial p_i}$ represents the sub-gradient of the cost function. The symbol $\bar{u}$ refers to the average node voltage, and u_{ref} signifies the reference voltage value. It is evident that when the system reaches the steady-state under λ-consensus control, the condition $\lambda_1 = \lambda_2 = \cdots = \lambda_n$ is satisfied, indicating that optimal power dispatch is achieved.

However, both p_{loss} and p_{load} are actually functions of u; that is, $\frac{\partial p_{loss}}{\partial p_i} \neq 0$ and $\frac{\partial p_{load}}{\partial p_i} \neq 0$. The condition in (5) is not the optimal condition of the economic dispatch problem, but can only be called the suboptimal condition. In fact, the vast majority of models in existing distributed optimization research make such assumptions, and as a result, these methods cannot achieve global optimality [22].

In summary, to simplify the optimization model, existing distributed optimization methods ignore complex power flow characteristics, resulting in a deviation between the operating point and the optimal point. In this paper, a more accurate optimal power flow model is proposed by taking into account the characteristics of complex power flow.

2.2. The Optimization Model of DC Microgrid Considering Power Flow Constraints

Consider a generalized DC microgrid comprising n power nodes and m load nodes, which can be represented as a graph. The power sources and loads correspond to the graph's nodes, while the transmission lines are modeled as edges, with each line having an associated resistance. Let Y represent the admittance matrix, where the off-diagonal elements are defined as $y_{ij} = -\frac{1}{r_{ij}}$ if there is a line between nodes i and j (with r_{ij} being the line resistance), and $y_{ij} = 0$ otherwise. The diagonal elements are given by $y_{ii} = -\sum_j y_{ij}$. Assuming the graph is connected, any principal submatrix of Y is positive definite. The load nodes are modeled as constant impedance nodes, with R_L being the diagonal matrix whose diagonal elements correspond to the load resistances. Let $u \in \mathbb{R}+^n$ and $u_L \in \mathbb{R}+^m$ denote the voltages at the power and load nodes, respectively.

According to Kirchhoff's law and Ohm's law, we obtain

$$\begin{bmatrix} i \\ i_L \end{bmatrix} = Y \begin{bmatrix} u \\ u_L \end{bmatrix} = \begin{bmatrix} Y_{SS} & Y_{SL} \\ Y_{LS} & Y_{LL} \end{bmatrix} \begin{bmatrix} u \\ u_L \end{bmatrix} \tag{7}$$

$$i_L = -R_L^{-1} u_L \tag{8}$$

Combining (7) and (8), we obtain

$$i = \left(Y_{SS} - Y_{SL}(R_L^{-1} + Y_{LL})^{-1} Y_{LS} \right) u \tag{9}$$

Define $Y_{eq} = Y_{SS} - Y_{SL} \left(Y_{LL} + R_L^{-1} \right)^{-1} Y_{LS}$, we have

$$p = [u] Y_{eq} u \tag{10}$$

Since the admittance matrix Y is the Laplacian matrix [23] of a connected network, its principal submatrix is positive definite, and then $Y_{LL} + R_L^{-1}$ is positive definite and invertible.

The optimal power flow problem of DC microgrid considering voltage regulation can be described as the following form, denoted as OPF 1:

$$\begin{aligned} \min \ & \sum_{i=1}^{n} f_i(p_i) \\ s.t. \ & p = [u] Y_{eq} u \\ & 1_n^T u^2 = n u_{ref}^2 \\ & u \geq 0_n \end{aligned} \tag{11}$$

The constraints include power flow, voltage regulation, and non-negativity of the optimization variables. Therefore, the accurate optimization model of DC microgrid under distributed framework is derived.

The power flow constraints in OPF 1 are nonlinear equalities, which make the optimization problem non-convex. As a result, finding the optimal solution is challenging, especially for large-scale systems. This paper focuses on the following three questions:

Q1: Is there a convex relaxation method that can convert the original non-convex problem in (11) into a convex one while preserving the same optimal solution?

Q2: Can a consensus condition be derived from the optimality condition of the convexified problem and integrated into the distributed control strategy to ensure global optimality?

Q3: Given that achieving global optimality requires global information, which typically involves centralized communication, can a distributed control method be proposed that achieves the same result using only a sparse communication network?

3. The Proposed Distributed Cost Optimization Control Strategy on Convex Relaxation Method

3.1. The Proposed Convex Relaxation Technique

Since the power flow constraint is a quadratic equality, which is convex only when linear, we introduce a mapping to transform it into a linear equality constraint [24,25]. Specifically, we define a new variable $W \triangleq [w_{ij}]$, where the elements satisfy $w_{ii} = u_i^2$ and $w_{ij} = w_{ji} = u_i u_j$, i.e., $W = uu^T$. Then, the optimization problem in (11) can be transformed into the following form (denoted as OPF 2):

$$
\begin{aligned}
\min &\sum_{i=1}^{n} f_i(p_i) \\
s.t. \ p = &\begin{bmatrix} p_1 \\ p_2 \\ \vdots \\ p_n \end{bmatrix} = \begin{bmatrix} y_{11}w_{11} + y_{12}w_{12} \cdots + y_{1n}w_{1n} \\ y_{21}w_{21} + y_{22}w_{22} \cdots + y_{2n}w_{2n} \\ \vdots \\ y_{n1}w_{n1} + y_{n2}w_{n2} \cdots + y_{nn}w_{nn} \end{bmatrix} \\
&w_{11} + w_{22} + \cdots + w_{nn} = n^2 u_{ref}^2 \\
&\begin{bmatrix} w_{ii} & w_{ij} \\ w_{ij} & w_{jj} \end{bmatrix} \geq 0, rank\left(\begin{bmatrix} w_{ii} & w_{ij} \\ w_{ji} & w_{jj} \end{bmatrix} \right) = 1
\end{aligned}
\tag{12}
$$

In this way, the power flow constraint and the voltage regulation constraint become linear equality constraints. Since $\begin{bmatrix} w_{ii} & w_{ij} \\ w_{ji} & w_{jj} \end{bmatrix} \geq 0$ is also a convex constraint; hence, only $rank\left(\begin{bmatrix} w_{ii} & w_{ij} \\ w_{ji} & w_{jj} \end{bmatrix} \right) = 1$ is left as a non-convex constraint in the problem. By removing the rank-one constraint, the original non-convex optimization problem is relaxed into a convex problem as follows (denoted as ROPF 1):

$$
\begin{aligned}
\min &\sum_{i=1}^{n} f_i(p_i) \\
s.t. \ &p = \begin{bmatrix} y_1 w_1 & y_2 w_2 & \cdots & y_n w_n \end{bmatrix}^T \\
&w_{11} + w_{22} + \cdots + w_{nn} = n u_{ref}^2 \\
&\begin{bmatrix} w_{ii} & w_{ij} \\ w_{ij} & w_{jj} \end{bmatrix} \geq 0
\end{aligned}
\tag{13}
$$

where $Y_{eq} = \begin{bmatrix} y_1^T & y_2^T & \cdots & y_n^T \end{bmatrix}^T$, with y_i representing the i-th row vector of Y_{eq}, and $W = \begin{bmatrix} w_1 & w_2 & \cdots & w_n \end{bmatrix}$, where w_i denotes the i-th column vector of W.

Remark 1. *Although OPF 1 has been relaxed into a convex problem (ROPF 1), the feasible region of ROPF 1 is much larger than that of the original problem, meaning its optimal solution may not lie within the feasible region of OPF 1. We define the convex relaxation as exact if OPF 1 and ROPF 1 share the same global optimal solution.*

3.2. The Exactness of the Proposed the Proposed Convex Relaxation Technique

In this section, we prove that the proposed convex relaxation method is exact [26,27]. Specifically, the relaxation is exact if the optimal solution of ROPF 1 satisfies $rank\left(\begin{bmatrix} w_{ii} & w_{ij} \\ w_{ji} & w_{jj} \end{bmatrix}\right) = 1$, meaning that OPF 1 and ROPF 1 share the same optimal solution.

Note that $f_i(p_i)$ is a strictly increasing function of p_i. Since $p_i = \sum_{j=1}^{n} y_{ij} w_{ji}$, with $y_{ii} > 0$ and $y_{ij} \leq 0$, $f(p_i)$ increases with w_{ii} and decreases with w_{ij}. Therefore, $\sum_{i=1}^{n} f_i(p_i)$ achieves its minimum when w_{ii} is minimized and w_{ij} is maximized. This monotonicity proves the exactness of the convex relaxation method.

Theorem 1. *The optimal solution of ROPF 1 must satisfy that $\begin{bmatrix} w_{ii} & w_{ij} \\ w_{ji} & w_{jj} \end{bmatrix}$ is positive semi-definite and* $\text{rank}\left(\begin{bmatrix} w_{ii} & w_{ij} \\ w_{ji} & w_{jj} \end{bmatrix}\right) = 1$.

Proof. Let (W^*, p^*) denote the optimal solution of ROPF 1, and $\begin{bmatrix} w_{hh}^* & w_{hk}^* \\ w_{hk}^* & w_{kk}^* \end{bmatrix}$ is positive definite. We now demonstrate that there exists an alternative feasible solution $(\tilde{W}, \tilde{p})$ satisfying $\tilde{p} \leq p^*$ and $f(\tilde{p}) < f(p^*)$.

Constructing the New Solution. Let $\tilde{w}_{hk} = w_{hk}^* + \varepsilon$, where ε is a small positive number satisfying $\left(w_{hk}^* + \varepsilon\right)^2 \leq w_{hh}^* w_{kk}^*$. This ensures that the modified matrix $\begin{bmatrix} w_{hh}^* & \tilde{w}_{hk} \\ \tilde{w}_{hk} & w_{kk}^* \end{bmatrix}$ remains positive semi-definite, maintaining the feasibility of the solution with respect to any constraints involving this submatrix. Let the remaining elements of $\tilde{W}$ be identical to those in W^*, so only $\tilde{w}_{hk}$ is modified from W^*. With this construction, it is straightforward to verify that $(\tilde{W}, \tilde{p})$ satisfies all the constraints of ROPF 1, and thus, it is a feasible solution to ROPF 1.

Comparing Objective Values. Define $\tilde{p} = [y_1 \tilde{w}_1, \cdots, y_n \tilde{w}_n]^T$. Since p_k and p_h are strictly decreasing with w_{hk}, increasing w_{hk}^* by ε leads to $\tilde{p}_h < p_h^*$ and $\tilde{p}_k < p_k^*$. For other indices $i \neq h, k$, $\tilde{p}_i = p_i^*$ because the corresponding elements of $\tilde{W}$ are unchanged. Since $f_i(p_i)$ is strictly increasing with p_i for all i, we obtain $\sum_{i=1}^{n} f_i(\tilde{p}_i) < \sum_{i=1}^{n} f_i(p_i^*)$. Therefore, the objective value at $(\tilde{W}, \tilde{p})$ is strictly less than that at (W^*, p^*).

This contradiction indicates that the optimal solution of ROPF 1 must satisfy that $\begin{bmatrix} w_{ii} & w_{ij} \\ w_{ji} & w_{jj} \end{bmatrix}$ is positive semi-definite and $\text{rank}\left(\begin{bmatrix} w_{ii} & w_{ij} \\ w_{ji} & w_{jj} \end{bmatrix}\right) = 1$. □

Remark 2. *Since ROPF 1 is a relaxation of OPF 1, their optimal values must satisfy $f_{ROPF1}^* \leq f^*$, where f^* is the optimal value of OPF 1. Theorem 1 shows that the point at which ROPF 1 attains its minimum also lies within the feasible region of OPF 1; then, we obtain $f_{ROPF1}^* = f^*$. Therefore, the first question Q1 is resolved.*

Remark 3. *The convex relaxation is often achieved by simplifying or relaxing nonlinear constraints, which can potentially lead to solutions that violate physical and operational limits. However, for OPF 1, we have proven that the convex relaxation is exact. This means that the optimal solution of the relaxed convex problem OPF 2 will always satisfy the original constraints. As a result, the obtained solution will not violate any physical or operational limits, ensuring the applicability of the method in practical scenarios.*

3.3. The Optimality Condition of OPF Problem in Distributed Framework

In this part, we derive the KKT conditions for ROPF 1. ROPF 1 can be expressed in the equivalent form (denoted as ROPF 2):

$$
\begin{aligned}
\min\ & \sum_{i=1}^{n} f_i(y_i w_i) \\
s.t.\ & w_{11} + w_{22} + \cdots + w_{nn} = nu_{ref}^2 \\
& w_{ii}w_{jj} \geq w_{ij}^2,\ w_{ii} > 0
\end{aligned}
\tag{14}
$$

The Lagrangian function of (14) is given by

$$
\begin{aligned}
L(W, \lambda, \mu, \nu) = & \sum_{i=1}^{n} f_i(y_i w_i) \\
& + \lambda \left(w_{11} + w_{22} + \cdots + w_{nn} - nu_{ref}^2 \right) \\
& + \sum_{j \neq i} \mu_{ij} \left(w_{ij}^2 - w_{ii}w_{jj} \right) - \sum_{i=1}^{n} \nu_i w_{ii}
\end{aligned}
\tag{15}
$$

where λ, μ_{ij}, and ν_i are Lagrange multipliers. The partial derivatives of $L(W, \lambda, \mu, \nu)$ with respect to W are given by

$$
\frac{\partial L}{\partial w_{ii}} = g_i(p_i)y_{ii} + \lambda - \sum_{j \neq i} \mu_{ij}w_{jj} - \nu_i
\tag{16}
$$

$$
\frac{\partial L}{\partial w_{ij}} = g_i(p_i)y_{ij} + g_j(p_i)y_{ij} + 2\mu_{ij}w_{ij}
\tag{17}
$$

where $g_i(p_i) = \frac{\partial f_i}{\partial p_i} = 2a_i y_i w_i + b_i$. Then, the KKT conditions of ROPF 2 are obtained as

$$
\begin{cases}
g_i(p_i)y_{ii} + \lambda - \sum_{j \neq i} \mu_{ij}w_{jj} - \nu_i = 0 \\
g_i(p_i)y_{ij} + g_j(p_i)y_{ij} + 2\mu_{ij}w_{ij} = 0 \\
w_{11} + w_{22} + \cdots + w_{nn} = nu_{ref}^2 \\
w_{ij}^2 \leq w_{ii}w_{jj} \\
\mu_{ij} \geq 0 \\
\mu_{ij}\left(w_{ij}^2 - w_{ii}w_{jj} \right) = 0 \\
\nu_i \geq 0 \\
w_{ii} > 0 \\
\nu_i w_{ii} = 0
\end{cases}
\tag{18}
$$

Since both ROPF 2 and ROPF 1 are convex, the KKT conditions are necessary and sufficient for optimality, ensuring a unique global optimal solution. When ROPF 1 reaches its optimal solution, $w_{ii} > 0$ must hold, and therefore its corresponding multiplier is 0, i.e., $\nu_i = 0$. At the same time, $w_{ij}^2 = w_{ii}w_{jj}$ must hold according to Theorem 1. Substituting $w_{ij} = u_i u_j$ and $w_{ii} = u_i^2$ into (18), the KKT condition can be simplified as

$$
\begin{cases}
g_i(p_i)y_{ii} + \lambda - \sum_{j \neq i} \mu_{ij}u_j^2 = 0 \\
(g_i(p_i) + g_j(p_j))y_{ij} + 2\mu_{ij}u_i u_j = 0 \\
u_1^2 + u_2^2 + \cdots + u_n^2 = nu_{ref}^2 \\
\mu_{ij} \geq 0
\end{cases}
\tag{19}
$$

Substituting $\mu_{ij} = -\frac{y_{ij}(g_i(p_i)+g_j(p_j))}{2u_iu_j}$ into the first equation in (19), it becomes

$$\begin{cases} x_1 = x_2 = \cdots = x_n = -\lambda \\ x_i = \dfrac{1}{2u_i}(g_i \displaystyle\sum_{j=1}^{n} y_{ij}u_j + \sum_{j=1}^{n} y_{ij}u_j g_j(p_j)) \\ u_1^2 + u_2^2 + \cdots + u_n^2 = nu_{ref}^2 \end{cases} \quad (20)$$

Notice that $i_i = \sum_{j=1}^{n} y_{ij}u_j$, then x_i becomes

$$x_i = \frac{1}{2u_i}(g_i(p_i)i_i + \sum_{j=1}^{n} y_{ij}u_j g_j(p_j)) \quad (21)$$

The (20) is the equivalent "consensus" form of the KKT conditions for OPF 1. To achieve (20) in the steady-state, the distributed consensus control method is designed as follows

$$\dot{u} = -Lx + \left(u_{ref}^2 - \bar{u}\right)1_n \quad (22)$$

where $\bar{u} = \frac{1}{n}\sum_{j=1}^{n} u_j^2$ and L is the Laplacian matrix of the communication network. The first term in the above distributed control method is the synchronization term that ensures $x_1 = x_2 = \cdots = x_n$ at the steady-state. The second item is the voltage regulation item. These two terms together form the sufficient and necessary conditions of KKT for the optimal solution of power flow, so the system can achieve global optimization at the steady-state if x_i can be obtained through the communication network. A distinct advantage of the proposed method in (22) is that the system will operate automatically at the global optimal point, eliminating the need to use interior-point methods to solve the optimization problem ROPF 1. Therefore, the second problem Q2 has been addressed.

However, since $Y_{LL} + R_L^{-1}$ is a irreducible M-matrix, $(Y_{LL} + R_L^{-1})^{-1}$ consists entirely of positive elements, which results in all elements of Y_{eq} being non-zero ($y_{ij} \neq 0$ for all i, j). Therefore, x_i relies on global information, specifically requiring knowledge of all line impedances, load resistances, voltages at the source nodes, and cost parameters. From this perspective, the implementation of (22) necessitates a centralized communication network to obtain the global information, which may lead to high communication cost. Next, we will propose a distributed observer to acquire global information, allowing the distributed optimization control method in (22) to be implemented through a low-bandwidth sparse communication network.

Remark 4. *Solving large-scale SOCP problems is indeed challenging although it is convex. For the network with n nodes, the original problem involves n voltage variables (u_i), but after SOCP relaxation, the number of variables (w_{ij}) increases to $n(n+1)/2$, which significantly increases the computational burden. However, the core idea of this paper is to derive the KKT conditions of the convex optimization problem and transform them into a consensus form (see Equation (20)). By utilizing distributed consensus control, the system automatically operates at the optimal point when the optimal factors x_i are consensus, eliminating the need to solve the optimization problem directly. Therefore, the proposed approach effectively addresses the scalability issue of SOCP.*

3.4. The Proposed Distributed Cost Optimization Control Strategy with Distributed Observers

The sparse communication network that communicates only with a few neighboring nodes is more suitable for DC microgrids with many distributed power sources.

In x_i, all the line resistances and loads are assumed to be known, then y_{ij} is available for any i and j. i_i, u_i and $g_i(p_i)$ are local variables, while the term $\sum_{j=1}^{n} y_{ij}u_j g_j(p_j)$ involves global

variables. Moreover, for the voltage regulation term, $\bar{u}$ is also contains global variables. The general distributed average state observer is proposed as follows

$$\varphi = z + \frac{1}{\varepsilon} \int -L\varphi dt, \varphi(0) = 0_n \tag{23}$$

where z is the input to the distributed average state observer, which is used to observe its average value. ε is a small positive scalar. φ is the estimate of average value of z, which satisfies

$$\lim_{t \to +\infty} \left(\varphi_i(t) - \frac{1}{n} \sum_{j=1}^{n} z_j(t) \right) = 0 \tag{24}$$

In the proposed distributed optimal control method, there are $n + 1$ average state variables need to be observed, namely, $\bar{u}$, $m_i = [u][g(p)]y_i^T, i \in 1, 2, \ldots, n$, where y_i^T is the i-th column vector of Y_{eq}, and $g(p) = [g_1(p_1), g_2(p2), \ldots, g_n(p_n)]^T$.

For $\bar{u}$, the distributed average state observer is designed as

$$\hat{u} = -\frac{1}{\varepsilon} \int L\hat{u} dt + u^2 \tag{25}$$

For m_i, the distributed average state observer is designed as

$$\hat{m}_i = -\frac{1}{\varepsilon} \int L\hat{m}_i dt + m_i \tag{26}$$

Then, the distributed optimal control method with distributed average state observers are as follows.

$$\dot{u}_i = \sum a_{ij} \left(\frac{1}{u_i}(g_i(p_i)i_i + n\alpha_i) - \frac{1}{u_j}(g_j(p_j)i_j + n\alpha_j) \right) \\ + (u_{ref}^2 - \hat{u}_i) \tag{27}$$

where a_i is an arbitrary element of m_i.

Remark 5. *To achieve global optimality, global information is necessary; however, such information is generally difficult to obtain directly through sparse communication networks. This paper implements the observation of global information through $n + 1$ distributed average state observers, enabling the proposed distributed optimization method to be applied in a sparse communication network. Hence, Q3 is addressed.*

3.5. Stability Analysis

3.5.1. The Small-Signal Model of the System Based on Singular Perturbation Theory

Due to the presence of the distributed observers, the order of the whole system is high and the stability is difficult to analysis. To simplify the stability analysis, we assume ε is sufficient small. Then, the system will exhibit significant multi-time-scale characteristics; the reduced-order system is given in (22) while the bound-layer system is given in (23). Clearly, the bound-layer system mainly corresponds to the dynamics of the distributed observer while the reduced-order system corresponds to the dynamics of the system under the distributed optimal control.

The small-signal model of the reduced-order system is given by

$$\Delta\dot{u} = -\left(\frac{2}{n}1_n 1_n^T[u^*] + L\frac{\partial x}{\partial u}(u^*)\right)\Delta u \tag{28}$$

where u^* is the equilibrium of the system. The small-signal model of the bound-layer system is given by

$$\Delta\dot{\varphi} = -\frac{1}{\varepsilon}L\Delta\varphi, \Delta\varphi = \Delta\hat{u}, \Delta\hat{m}_1, \Delta\hat{m}_2, \ldots, \hat{m}_n \tag{29}$$

Then, main results are as follows.

Theorem 2. *If the eigenvalue of $\frac{2}{n}1_n1_n^T[u^*] + L\frac{\partial x}{\partial u}(u^*)$ has positive real parts, then there exists a positive scalar ε^* such that the system is stable when $0 < \varepsilon \leq \varepsilon^*$.*

Proof. According to the singular perturbation theorem, if both the reduced-order and boundary-layer systems are stable, there exists a positive scalar ε^* such that the original system is stable for $0 < \varepsilon < \varepsilon^*$. It can be easily shown that the reduced-order system is stable if $\frac{2}{n}1_n1_n^T[u^*] + L\frac{\partial x}{\partial u}(u^*)$. Based on the findings in [28], the boundary-layer system is inherently stable. Thus, Theorem 2 is validated. $\square$

Theorem 2 provides the stability conditions for the system under the proposed distributed control strategy, thereby ensuring that the control strategy can effectively achieve the goals of voltage recovery and power flow optimization. ε^* in Theorem 2 can be calculated using numerical methods such as the root locus method. It will be set to an appropriate value within the stable range in the simulation, and the stability of the control strategy will be verified under sudden load changes.

3.5.2. Stability Analysis of the System Under Communication Delays

Sparse communication networks often have certain delays, so it is necessary to study the impact of communication delays on system stability. Let τ denote the communication delay, then the small-signal models of the reduced-order system and bound-layer system with delays are given by

$$\Delta\dot{u} = -(\frac{2}{n}1_n1_n^T[u^*] + L\frac{\partial x}{\partial u}(u^*))\Delta u(t - \tau) \tag{30}$$

$$\Delta\dot{\varphi} = -\frac{1}{\varepsilon}L\Delta\varphi(t - \tau) \tag{31}$$

The characteristic equations of the above systems are given by

$$|sI + (\frac{2}{n}1_n1_n^T[u^*] + L\frac{\partial x}{\partial u}(u^*))e^{-\tau s}| = 0 \tag{32}$$

$$|sI + \frac{1}{\varepsilon}Le^{-\tau s}| = 0 \tag{33}$$

Let $\lambda_2 \leq \lambda_3 \leq \cdots \leq \lambda_n$ be the non-zero eigenvalues of L, $r_1e^{\theta_1 j}, r_2e^{\theta_2 j}, \ldots, r_ne^{\theta_n j}$ be the eigenvalues of $\frac{2}{n}1_n1_n^T[u^*] + L\frac{\partial x}{\partial u}(u^*)$. Then, main results are as follows:

Theorem 3. *If the eigenvalue of $\frac{2}{n}1_n1_n^T[u^*] + L\frac{\partial x}{\partial u}(u^*)$ has positive real parts, then the system is stable if and only if $0 < \tau < \tau^*$ where*

$$\tau^* = min\left\{\frac{\varepsilon\pi}{2\lambda_n}, \frac{\pi - 2|\theta_1|}{2r_1}, \frac{\pi - 2|\theta_2|}{2r_2}, \ldots, \frac{\pi - 2|\theta_n|}{2r_n}\right\} \tag{34}$$

Proof. The necessary and sufficient condition for system stability is that the roots of the transcendental equations in (31) and (32) all have negative real parts. Theorems (32) and (33) are equivalent to (35) and (36), respectively.

$$\prod_{i=1}^{n}(s + r_ie^{\theta_i j}e^{-\tau s}) = 0 \tag{35}$$

$$s(s + \lambda_2e^{-\tau s})\ldots(s + \lambda_ne^{-\tau s}) = 0 \tag{36}$$

Then, the system is stable if and only if the roots of all sub-equations ($s + r_ie^{\theta_i j}e^{-\tau s} = 0$ and $s + \lambda_ne^{-\tau s} = 0$) are located in the left half-plane. By invoking the existing results

(Theorem 4 in [29]), the roots of $s + r_i e^{\theta_{ij}} e^{-\tau s} = 0$ are located in the left half-plane if and only if

$$\tau r_i + |\theta_i| < \frac{\pi}{2} \tag{37}$$

Likewise, the roots of (36) has negative real parts if and only if

$$\tau < min\left\{\frac{\varepsilon\pi}{2\lambda_2}, \frac{\varepsilon\pi}{2\lambda_3}, \cdots, \frac{\varepsilon\pi}{2\lambda_n}\right\} = \frac{\varepsilon\pi}{2\lambda_n} \tag{38}$$

Combine (37) and (38), (34) is obtained, thus proving Theorem 3. □

Since the eigenvalue of $\frac{2}{n}1_n 1_n^T[u^*] + L\frac{\partial x}{\partial u}(u^*)$ has positive real parts, which implies $|\theta_i| < \frac{\pi}{2}$, there exists a positive scalar ε^* that satisfies (34). On the other hand, ε should be sufficient small to ensure the acceptable convergence rate of the distributed observers. However, it will decrease the maximal communication delay that keep the system stable. Since ε^* is small, τ^* can be regarded as $\tau^* = \frac{\varepsilon\pi}{2\lambda_n}$.

4. Case Studies

To verify the proposed method, a DC microgrid based on the IEEE 10-bus system is designed, as shown in Figure 1. In this diagram, red nodes denote sources, purple nodes represent loads, and node numbers are labeled in black. The cables are represented by black solid lines, with the resistance values indicated by red numbers.
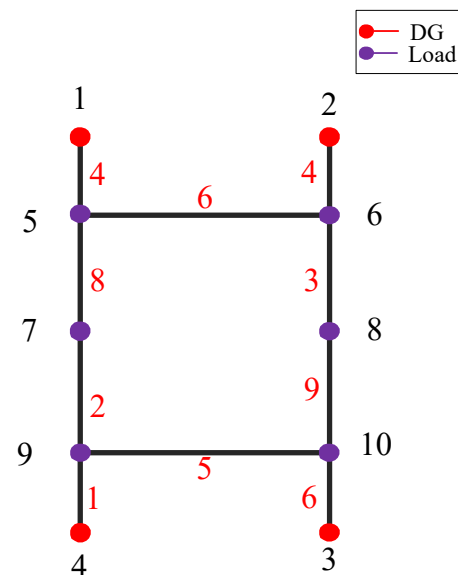
Figure 1. The topology of the DC microgrid with 10 nodes.

Parameter designing. For A 10-node DC microgrid system, set the parameter values of $u_{ref} = 48$ V and the objective function $f_i(p_i) = a_i p_i^2 + b_i p_i + c_i$ as $a = [2, 1, 0.5, 0.1]^T$, $b = [10, 20, 5, 10]^T$, $c = [0, 0, 0, 0]^T$. $R_L = [10, 20, 10, 30, 20, 30]$. $\varepsilon = 0.1$.

The Laplacian matrix of the communication network is given by

$$L = \begin{bmatrix} 2 & -1 & 0 & -1 \\ -1 & 2 & -1 & 0 \\ 0 & -1 & 2 & -1 \\ -1 & 0 & -1 & 2 \end{bmatrix}$$

4.1. Optimality Verification

This section aims to assess whether the proposed distributed control method can achieve global optimization. The MATLAB 2018b, CVX Optimization Toolbox is used

to compute the global optimal solution of the convex problem ROPF 2. If the system's steady-state under the proposed control method aligns with the global optimal solution obtained via the MATLAB 2018b CVX Optimization Toolbox, it confirms that the method ensures global optimal operation of the system.

The calculation results from the MATLAB CVX Optimization Toolbox are shown. Here, the CVX built-in optimization solver MOSEK is used to solve, the core algorithm of which is the interior-point method. Results show that the objection function converges to the minimum value 156,708,898.75 and the global solution is

$$W = \begin{bmatrix} 2016.5 & 2053.2 & 2270.9 & 2281.3 \\ 2053.2 & 2090.6 & 2312.2 & 2322.7 \\ 2270.9 & 2312.2 & 2557.4 & 2569.0 \\ 2281.3 & 2322.7 & 2569.0 & 2580.7 \end{bmatrix} \tag{39}$$

which is equivalent to u = [44.9060, 45.7228, 50.5705, 50.8007] V. The iterative convergence process are presented in Figure 2, which shows that the voltage in the steady-state coincides with the global optimal solution obtained by the MATLAB CVX optimization toolkit. Therefore, simulation results verifies that the proposed distributed control method can achieve global optimal operation of the system.
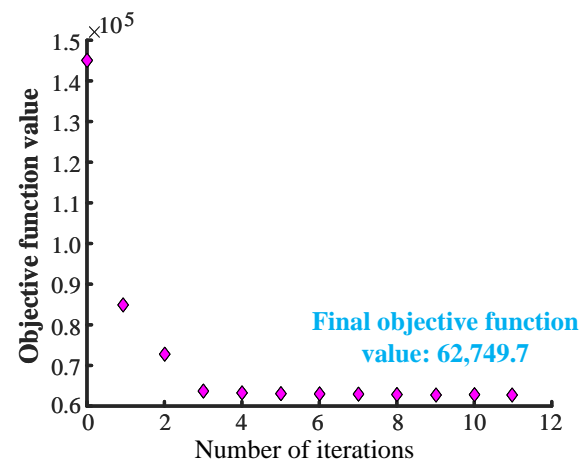
Figure 2. Convergence iterative process for power flow optimization of the 10-node DC microgrid.

4.2. Comparisons with Existing Distributed Optimization Control Methods

In related existing works about distributed optimal control [14], the convexification of the problem mainly relies on ignoring the flow constraints, while the proposed distributed control is primarily based on the equal incremental rate criterion, i.e., $\frac{\partial f_1(p_1)}{\partial p_1} = \frac{\partial f_2(p_2)}{\partial p_2} = \cdots = \frac{\partial f_n(p_n)}{\partial p_n}$.

Based on the 10-node DC microgrid system, Figure 3 and Figure 4, respectively, show the voltage waveform of each micro-source node of the system based on the control strategy in this chapter and the comparison control strategy. The simulation results of the system under the distributed control proposed in [14] are presented in Figure 4. In this comparison simulation, only x_i is replaced with $\frac{\partial f_i(p_i)}{\partial p_i}$, while all other parameters remain unchanged. Simulation results comparing the proposed method and the existing method in [14] are presented in Table 1. Results show that the steady-state voltages of DGs under the existing distributed control are u = [44.9060, 45.7227, 50.5705, 50.8006] V and the objective function is 65,509.4, while it is 62,749.3 in the proposed method. Therefore, simulation results verify that the minimum value obtained proposed method is lower than the existing method.
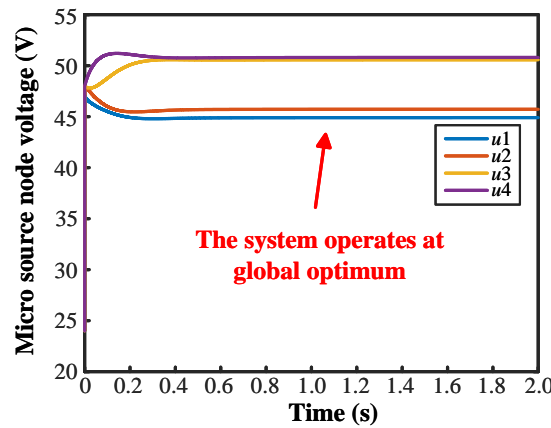
Figure 3. The voltage waveform of the 10-node DC microgrid based on the proposed method.
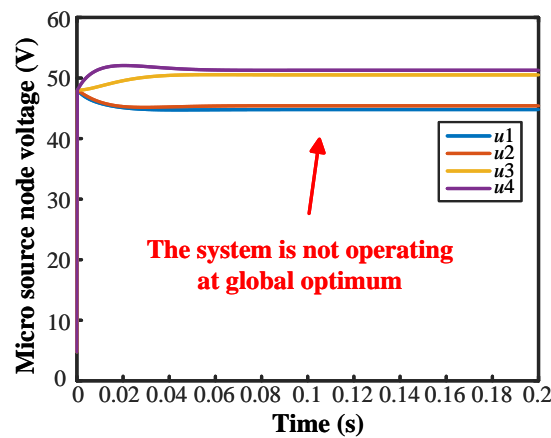

Figure 4. The voltage waveform of the 10-node DC microgrid based on the existing method in [14].

Table 1. Comparison of simulation operation control strategies for 10-node DC microgrid.

Control Strategy	The Proposed Method	The Method in [14]
Voltage vector u	u	v
Optimal factor vector x	x	λ
Total cost function steady-state value	62,749.3	65,509.4
Is the voltage recovery condition met?	Yes	Yes
Is the optimal factor consistency condition satisfied?	Yes	No
Is the steady-state solution optimal?	Yes	No
Is the steady-state value of the total cost function optimal?	Yes	No

$u = [44.9060, 45.7227, 50.5705, 50.8006]^T$ V. $v = [44.7902, 45.4157, 50.5194, 51.2889]^T$ V. $x = [3.1730, 3.1730, 3.1730, 3.1730]^T$.
$\lambda = [137.58, 137.58, 137.58, 137.58]^T$.

4.3. Stability of the System Under Communication Delays

To verify the impact of communication delays on the system stability, we introduce appropriate delay modules into the simulated communication links. According to Theorem 3, if the eigenvalues of $(\frac{2}{n}1_n1_n^T[u^*] + L\frac{\partial x}{\partial u}(u^*))$ have positive real parts, then the system is stable if and only if $0 < \tau < \tau^*$. By calculation, the eigenvalue of $(\frac{2}{n}1_n1_n^T[u^*] + L\frac{\partial x}{\partial u}(u^*))$ is 15.11, 2.16, 2.50, and 3.36. The eigenvalues of its Laplacian matrix are $\lambda_1 = 0$, $\lambda_2 = \lambda_3 = 2$, and $\lambda_4 = 4$, and ε^* is obtained as $\tau^* = \frac{\varepsilon\pi}{2\lambda_4} = \frac{25\pi}{2} \approx 39.27$ ms. To test the correctness of Theorem 3, two scenarios are designed $\tau = 30$ ms and $\tau = 50$ ms. Clearly, the system will be stable when $\tau = 30$ ms and unstable when $\tau = 50$ ms.

Simulation results for the case $\tau = 30$ ms are presented in Figure 5a shows that the voltage waveforms of each micro-source node show little difference compared to the case

without communication delay, indicating that it has no significant impact on the node voltages when $\tau < \tau^*$. The dynamics of the optimal factors are presented in Figure 5b. It can be seen that the waveforms of the optimal factors exhibit noticeable fluctuations, and they reach the steady-state around 0.8 s, indicating that communication delays will slow down the convergence rate of the proposed method, though they do not affect the steady-state. Hence, simulation results verify that the system is stable if $\tau < \tau^*$.
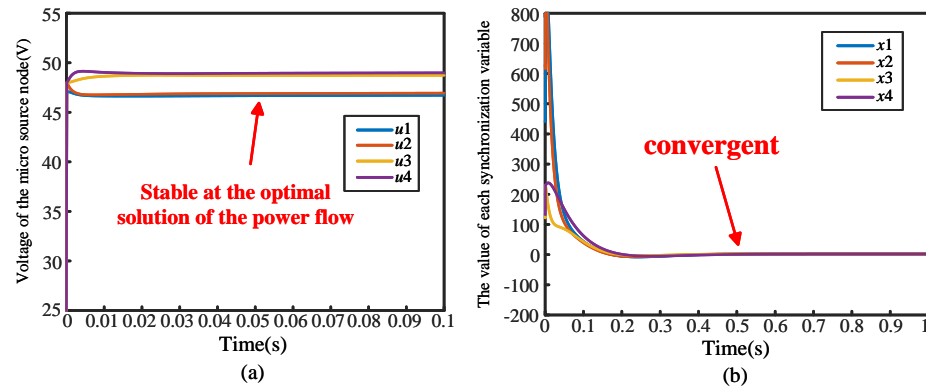
Figure 5. Simulation results under the communication delay τ = 30 ms. (**a**) The voltage waveform of each DG node. (**b**) The waveform of each optimal factor.

Simulation results for the case $\tau = 50$ ms are presented in Figure 6b shows that the time delay causes instability in the distributed observers, leading to a divergent oscillatory state in the optimal factors as well. Consequently, as shown in Figure 6a, this divergent oscillation in the optimal factors causes the DG voltages to oscillate as well. Hence, simulation results verify that the system is unstable when $\tau > \tau^*$.

In summary, simulation results show that the system is stable if and only if $\tau < \tau^*$, which verify the correctness of Theorem 3.
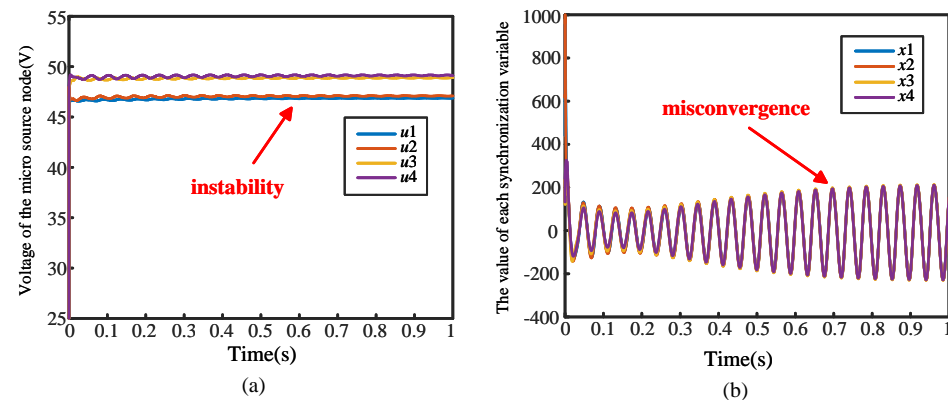
Figure 6. Simulation results under the communication delay τ = 50 ms. (**a**) The voltage waveform of each DG node. (**b**) The waveform of each optimal factor.

4.4. Performance Under Load Changes

This part is designed to test whether the proposed method can achieve global optimization under load changes. Here, load changes are designed at $t = 1$ s and $t = 2$ s. As can be seen from the simulation results in Figure 7, when the load changes abruptly, the optimal factors are inconsistent, which means that the system does not work at the optimal point. However, soon the optimal factors resynchronize and the system returns to the optimal operating point. Therefore, the proposed method can achieve global optimization under load variation without re-solving the power flow problem.
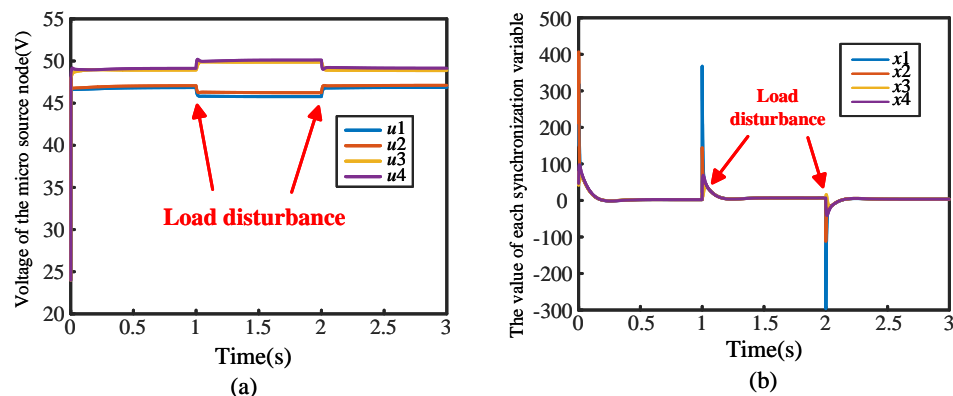
Figure 7. Simulation results under load variations. (**a**) The voltage waveform of each DG node. (**b**) The waveform of each optimal factor.

5. Conclusions

This paper presents a distributed optimization control strategy for DC microgrids that addresses the challenges of voltage recovery and optimal power flow scheduling. First, a semi-definite programming convex relaxation technique is developed to transform the inherently non-convex optimal power flow problem into a convex form, with proof of exactness ensuring consistency with the original problem.

Second, the KKT conditions are derived and reformulated as a synchronization term, enabling integration into distributed control for achieving optimal power flow. Third, to reduce communication costs associated with acquiring global information, a distributed observer-based control strategy is introduced. This innovation allows the control system to calculate optimal factors with a sparse communication network, thus making voltage restoration and global scheduling feasible even under limited connectivity.

The proposed distributed control strategy using convex relaxation techniques offers advantages in mathematical tractability and global optimality. However, it has limitations in handling complex physical constraints, discrete control variables, and scalability for large systems. Two key limitations should be noted: the method assumes linear loads, limiting its application to nonlinear load systems, and it relies on real-time load data, which poses practical challenges. Future work will focus on hybrid algorithms that combine convex relaxation with Mixed-Integer Programming (MIP) to handle discrete variables, and explore distributed optimization and parallel computing to improve scalability. Future research will address these issues by adapting the approach for the optimization model for more practical constraints and nonlinear loads.

In summary, this work contributes a scalable and cost-effective distributed control approach for DC microgrid optimization, paving the way for enhanced practical applications in energy management and distributed power systems.

References

1. Al-Ismail, F.S. DC microgrid planning, operation, and control: A comprehensive review. *IEEE Access* **2021**, *9*, 36154–36172. [CrossRef]
2. Ito, Y.; Zhongqing, Y.; Akagi, H. DC microgrid based distribution power generation system. In Proceedings of the The 4th International Power Electronics and Motion Control Conference (IPEMC 2004), Xi'an, China, 14–16 August 2004; Volume 3, pp. 1740–1745.
3. Zhou, S.; Chen, C.; Jin, Y.; Su, J.; Wei, T.; He, J.; Wang, Y. A review of dc power distribution system protection technology. *Proc. CSEE* **2014**, *34*, 3114–3122. [CrossRef]
4. Ensermu, G.; Bhattacharya, A.; Panigrahy, N. Real-time simulation of smart DC microgrid with decentralized control system under source disturbances. *Arab. J. Sci. Eng.* **2019**, *44*, 7173–7185. [CrossRef]
5. Liu, Z.; Liu, R.; Zhang, X.; Su, M.; Sun, Y.; Han, H.; Wang, P. Feasible Power-Flow Solution Analysis of DC Microgrids Under Droop Control. *IEEE Trans. Smart Grid* **2020**, *11*, 2771–2781. [CrossRef]
6. Tsikalakis, A.G.; Hatziargyriou, N.D. Centralized control for optimizing microgrids operation. In Proceedings of the 2011 IEEE Power and Energy Society General Meeting, Detroit, MI, USA, 24–28 July 2011; pp. 1–8.
7. Halilbašić, L.; Pinson, P.; Chatzivasileiadis, S. Convex Relaxations and Approximations of Chance-Constrained AC-OPF Problems. *IEEE Trans. Power Syst.* **2019**, *34*, 1459–1470. [CrossRef]
8. Wang, C.; Cui, B.; Wang, Z.; Gu, C. SDP-Based Optimal Power Flow With Steady-State Voltage Stability Constraints. *IEEE Trans. Smart Grid* **2019**, *10*, 4637–4647. [CrossRef]
9. Cui, B.; Sun, X.A. A New Voltage Stability-Constrained Optimal Power-Flow Model: Sufficient Condition, SOCP Representation, and Relaxation. *IEEE Trans. Power Syst.* **2018**, *33*, 5092–5102. [CrossRef]
10. Kumar, R.; Singh, R.; Ashfaq, H. Stability enhancement of multi-machine power systems using Ant colony optimization-based static Synchronous Compensator. *Comput. Electr. Eng.* **2020**, *83*, 106589. [CrossRef]
11. Swarnkar, K.; Wadhwani, S.; Wadhwani, A. Optimal Power Flow of large distribution system solution for Combined Economic Emission Dispatch Problem using Partical Swarm Optimization. In Proceedings of the 2009 International Conference on Power Systems, Kharagpur, India, 27–29 December 2009; pp. 1–5. [CrossRef]
12. Salimon, S.A.; Omofuma, O.I.; Akinrogunde, O.O.; Thomas, T.G.; Edwin, T.E. Optimal allocation of shunt capacitors in radial distribution networks using Constriction-Factor Particle Swarm Optimization and its techno-economic analysis. *Frankl. Open* **2024**, *7*, 100093. [CrossRef]
13. Pan, X.; Chen, M.; Zhao, T.; Low, S.H. DeepOPF: A Feasibility-Optimized Deep Neural Network Approach for AC Optimal Power Flow Problems. *IEEE Syst. J.* **2023**, *17*, 673–683. [CrossRef]
14. Li, Q.; Gao, D.W.; Zhang, H.; Wu, Z.; Wang, F.y. Consensus-Based Distributed Economic Dispatch Control Method in Power Systems. *IEEE Trans. Smart Grid* **2019**, *10*, 941–954. [CrossRef]
15. Tang, Z.; Hill, D.J.; Liu, T. A Novel Consensus-Based Economic Dispatch for Microgrids. *IEEE Trans. Smart Grid* **2018**, *9*, 3920–3922. [CrossRef]
16. Guo, F.; Wen, C.; Mao, J.; Song, Y.D. Distributed Economic Dispatch for Smart Grids With Random Wind Power. *IEEE Trans. Smart Grid* **2016**, *7*, 1572–1583. [CrossRef]
17. Ullah, M.H.; Park, J.D. Distributed Energy Optimization in MAS-based Microgrids using Asynchronous ADMM. In Proceedings of the 2019 IEEE Power & Energy Society Innovative Smart Grid Technologies Conference (ISGT), Washington, DC, USA, 18–21 February 2019; pp. 1–5. [CrossRef]
18. Xing, H.; Lin, Z.; Fu, M. An ADMM + consensus based distributed algorithm for dynamic economic power dispatch in smart grid. In Proceedings of the 2015 34th Chinese Control Conference (CCC), Hangzhou, China, 28–30 July 2015; pp. 9048–9053. [CrossRef]
19. Binetti, G.; Davoudi, A.; Lewis, F.L.; Naso, D.; Turchiano, B. Distributed consensus-based economic dispatch with transmission losses. *IEEE Trans. Power Syst.* **2014**, *29*, 1711–1720. [CrossRef]
20. Hou, X.; Sun, Y.; Lu, J.; Zhang, X.; Koh, L.H.; Su, M.; Guerrero, J.M. Distributed Hierarchical Control of AC Microgrid Operating in Grid-Connected, Islanded and Their Transition Modes. *IEEE Access* **2018**, *6*, 77388–77401. [CrossRef]
21. Morstyn, T.; Hredzak, B.; Demetriades, G.D.; Agelidis, V.G. Unified Distributed Control for DC Microgrid Operating Modes. *IEEE Trans. Power Syst.* **2016**, *31*, 802–812. [CrossRef]
22. Han, H.; Hou, X.; Yang, J.; Wu, J.; Su, M.; Guerrero, J.M. Review of Power Sharing Control Strategies for Islanding Operation of AC Microgrids. *IEEE Trans. Smart Grid* **2016**, *7*, 200–215. [CrossRef]
23. Liu, Z.; Su, M.; Sun, Y.; Yuan, W.; Han, H.; Feng, J. Existence and stability of equilibrium of DC microgrid with constant power loads. *IEEE Trans. Power Syst.* **2018**, *33*, 6999–7010. [CrossRef]
24. Gan, L.; Low, S.H. Optimal Power Flow in Direct Current Networks. *IEEE Trans. Power Syst.* **2014**, *29*, 2892–2904. [CrossRef]
25. Li, J.; Liu, F.; Wang, Z.; Low, S.H.; Mei, S. Optimal Power Flow in Stand-Alone DC Microgrids. *IEEE Trans. Power Syst.* **2018**, *33*, 5496–5506. [CrossRef]
26. Low, S.H. Convex Relaxation of Optimal Power Flow—Part I: Formulations and Equivalence. *IEEE Trans. Control Netw. Syst.* **2014**, *1*, 15–27. [CrossRef]
27. Low, S.H. Convex Relaxation of Optimal Power Flow—Part II: Exactness. *IEEE Trans. Control. Netw. Syst.* **2014**, *1*, 177–189. [CrossRef]

28. Olfati-Saber, R.; Murray, R.M. Consensus Problems in Networks of Agents With Switching Topology and Time-Delays. *IEEE Trans. Autom. Control* **2004**, *49*, 1520–1533. [CrossRef]
29. Liu, Z.; Su, M.; Sun, Y.; Han, H.; Hou, X.; Guerrero, J.M. Stability analysis of DC microgrids with constant power load under distributed control methods. *Automatica* **2018**, *90*, 62–72. [CrossRef]